Short-length and robust polarization rotators in periodically poled lithium niobate via shortcuts to adiabaticity

Xi Chen,[1,*] Hong-Wei Wang,[1] Yue Ban,[2] and Shuo-Yen Tseng[3,4,5]

[1]*Department of Physics, Shanghai University, 200444 Shanghai, China*
[2]*Department of Electronic Information Materials, Shanghai University, 200444 Shanghai, China*
[3]*Department of Photonics, National Cheng Kung University, Tainan, Taiwan*
[4]*Advanced Optoelectronic Technology Center, National Cheng Kung University, Tainan, Taiwan*
[5] *tsengsy@mail.ncku.edu.tw*
[*]*xchen@shu.edu.cn*

Abstract: Conventional narrowband spectrum polarization devices are short but not robust, based on quasi-phase matching (QPM) technique, in periodically poled lithium niobate (PPLN) crystal. In this paper, we propose short-length and robust polarization rotators by using shortcuts to adiabaticity. Beyond the QPM condition, the electric field and period of PPLN crystal are designed in terms of invariant dynamics, and further optimized with respect to input wavelength/refractive index variations. In addition, the stability of conversion efficiency on the electric field and period of PPLN crystal is also discussed. As a consequence, the optimal shortcuts are fast as well as robust, which provide broadband spectrum polarization devices with short length.

OCIS codes: (270.5585) Quantum information and processing; (190.4360) Nonlinear optics, devices; (260.1180) Crystal optics; (260.1440) Birefringence.

References and links

1. M. R. Watts and H. A. Haus, "Integrated mode-evolution-based polarization rotators," Opt. Lett. **30**, 138–140 (2005).
2. A. A. Rangelov, U. Gaubatz, and N. V. Vitanov, "Broadband adiabatic conversion of light polarization," Opt. Commun. **283**, 3891–3894 (2010).
3. A. A. Rangelov, "Achromatic polarization retarder realized with slowly varying linear and circular birefringence," Opt. Lett. **36**, 2716–2718 (2011).
4. S. S. Ivanov, A. A. Rangelov, N. V. Vitanov, T. Peters, and T. Halfmann, "Highly efficient broadband conversion of light polarization by composite retarders," J. Opt. Soc. Am. A **29**, 265–269 (2012).
5. S. Longhi, "Quantum-optical analogies using photonic structures," Laser and Photon. Rev. **3**, 243–261 (2009).
6. M. H. Levitt, "Composite pulses," Prog. Nucl. Magn. Reson. Spectrosc. **18**, 61–122 (1986).
7. X. Chen, A. Ruschhaupt, S. Schmidt, A. del Campo, D. Guéry-Odelin, and J. G. Muga, "Fast Optimal Frictionless Atom Cooling in Harmonic Traps: Shortcut to Adiabaticity," Phys. Rev. Lett. **104**, 063002 (2010).
8. X. Chen, I. Lizuain, A. Ruschhaupt, D. Guéry-Odelin, and J. G. Muga, "Shortcut to Adiabatic Passage in Two- and Three-Level Atoms," Phys. Rev. Lett. **105**, 123003 (2010).
9. S. Ibáñez, X. Chen, E. Torrontegui, J. G. Muga, and A. Ruschhaupt, "Multiple Schrödinger Pictures and Dynamics in Shortcuts to Adiabaticity," Phys. Rev. Lett. **109**, 100403 (2012).
10. E. Torrontegui, S. Ibáñez, S. Martínez-Garaot, M. Modugno, A. del Campo, D. Guéry-Odelin, A. Ruschhaupt, X. Chen, and J. G. Muga, "Shortcuts to adiabaticity," Adv. At. Mol. Opt. Phys. **62**, 117–169 (2013).
11. T.-Y. Lin, F.-C. Hsiao, Y.-W. Jhang, C. Hu, and S.-Y. Tseng, "Mode conversion using optical analogy of shortcut to adiabatic passage in engineered multimode waveguides," Opt. Express **20**, 24085–24092 (2012).

#220049 - $15.00 USD Received 29 Jul 2014; revised 8 Sep 2014; accepted 10 Sep 2014; published 25 Sep 2014

12. S.-Y. Tseng and X. Chen, "Engineering of fast mode conversion in multimode waveguides," Opt. Lett. **37**, 5118–5120 (2012).
13. S.-Y. Tseng, "Counterdiabatic mode-evolution based coupled-waveguide devices," Opt. Express **21**, 21224–21235 (2013).
14. S. Martínez-Garaot, S.-Y. Tseng, and J. G. Muga, "Compact and high conversion efficiency mode-sorting asymmetric Y junction using shortcuts to adiabaticity," Opt. Lett. **39**, 2306–2309 (2014).
15. S.-Y. Tseng, R.-D. Wen, Y.-F. Chiu, and X. Chen, "Short and robust directional couplers designed by shortcuts to adiabaticity," Opt. Express **22**, 18849—18859 (2014).
16. H. R. Lewis and W. B. Riesenfeld, "An exact quantum theory of the time-dependent harmonic oscillator and of a charged particle in a time-dependent electromagnetic field," J. Math. Phys. **10**, 1458–1473 (1969).
17. A. Ruschhaupt, X. Chen, D. Alonso, and J. G. Muga, "Optimally robust shortcuts to population inversion in two-level quantum systems," New J. Phys. **14**, 093040 (2012).
18. X.-J. Lu, X. Chen, A. Ruschhaupt, D. Alonso, S. Guérin, and J. G. Muga, "Fast and robust population transfer in two-level quantum systems with dephasing noise and/or systematic frequency errors," Phys. Rev. A **88**, 033406 (2013).
19. D. Daems, A. Ruschhaupt, D. Sugny, and S. Guérin, "Robust quantum control by a single-shot shaped pulse," Phys. Rev. Lett. **111**, 050404 (2013).
20. S. Thaniyavarn, "Wavelength-independent, optical-damage-immune $LiNbO_3$ TE-TM mode converter," Opt. Lett. **11**, 39–41 (1986).
21. Y.-Q. Lu, Z.-L. Wan, Q. Wang, Y.-X. Xi, and N.-B. Ming, "Electro-optic effect of periodically poled optical superlattice $LiNbO_3$ and its applications," Appl. Phys. Lett. **77**, 3719–3721 (2000).
22. Y.-M. Zhu, X.-F. Chen, J.-H. Shi, Y.-P. Chen, Y.-X. Xia, and Y.-L. Chen, "Wide-range tunable wavelength filter in periodically poled lithium niobate," Opt. Commun. **228**, 139–143 (2003).
23. K. Liu, J.-H. Shi, and X.-F. Chen, "Electro-optical flat-top bandpass Solc-type filter in periodically poled lithium niobate," Opt. Lett. **34**, 1051–1053 (2009).
24. K. Liu, J.-H. Shi, and X.-F. Chen, "Linear polarization-state generator with high precision in periodically poled lithium niobate," Appl. Phys. Lett. **94**, 101106 (2009).
25. K. Liu and X.-F. Chen, "Evolution of the optical polarization in a periodically poled superlattice with an external electric field," Phys. Rev. A **80**, 063808 (2009).
26. Y.-X. Zhang, Y.-P. Chen, and X.-F. Chen, "Polarization-based all-optical logic controlled-NOT, XOR, and XNOR gates employing electro-optic effect in periodically poled lithium niobate," Appl. Phys. Lett. **99**, 161117 (2011).
27. X.-J. Lu, J. G. Muga, X. Chen, U. G. Poschinger, F. Schmidt-Kaler, and A. Ruschhaupt, "Fast shuttling of a trapped ion in the presence of noise," Phys. Rev. A **89**, 063414 (2014).

1. Introduction

Design of polarizing devices has attracted much attention with applications in polarization splitting, rotation and retarder in optical communication and integrated optics for the last two decades [1–4]. However, these traditional devices face many unsolved issues, such as low conversion efficiency of output polarization, shift of central wavelength, and difficulty of miniaturization and integration because of the large volume of the optical components. Recently, the analogy between quantum mechanics and wave optics [5] provides alternative protocols, including adiabatic Landau-Zener scheme, to solve those problems, at least partially. For instance, the adiabatic polarization retarder is robust against variations of the propagation length, rotary power, but requires long propagation distance to satisfy the adiabatic condition [3]. In addition, the composite pulse scheme, originally proposed in nuclear magnetic resonance (NMR) [6], has been applied to design fast as well as robust polarization converters with highly efficient broadband conversion [4].

Recently, the techniques of "shortcuts to adiabaticity" (STA) [7–9] have been put forward to accelerate slow adiabatic quantum processes in the field of atom, molecular, and optical physics, see recent review [10]. In particular, STA provides the intriguing methods to design fast mode conversion and directional coupler in optical waveguide devices [11–15]. Among all the techniques, the inverse-engineering approach [7], based on Lewis-Riesenfeld invariant theory [16], provides a versatile toolbox for designing optimal shortcuts in presence of different types of noise and systematic errors, by combining time-dependent perturbation theory and optimal control theory [17–19]. This can be directly utilized to design short-length directional

#220049 - $15.00 USD Received 29 Jul 2014; revised 8 Sep 2014; accepted 10 Sep 2014; published 25 Sep 2014

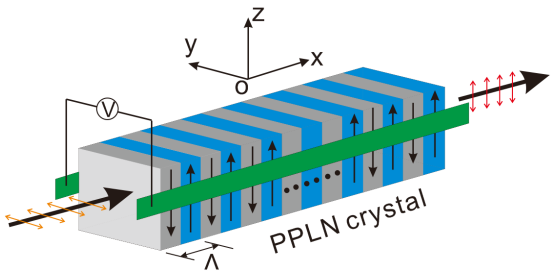

Fig. 1. Schematic diagram of polarization rotators in a PPLN crystal, where the electric field E is applied by voltage V, and Λ is the period of PPLN crystal.

couplers that are also robust against input wavelength/couple coefficient variations [15].

In this paper, we will apply STA to design the short-length and robust polarization rotators in the ferroelectric crystals under external electric field. As a matter of fact, an electro-optic polarization converter, e.g. $LiNbO_3$ waveguide, has been already proposed in 1980s, with the applications in single-mode fabric-optic systems [20], since the phase matching and coupling strength can be easily adjusted by electro-optic effect. Later on, the periodically poled lithium niobate (PPLN) and periodically poled lithium tantalate (PPLT) have been investigated theoretically and experimentally [21–26] for optical polarization state control with applications in wavelength filter, electro-optic switch, polarization-state generator, and even optical logic gates. Most of above applications in PPLN crystals are based on the so-called quasi-phase-matched (QPM) technology, but such resonant scheme of polarization state manipulations in PPLN is sensitive to wavelength variation, when the condition for QPM is satisfied. Thus, beyond the QPM condition, the polarization state control becomes interesting and important, especially when the QPM wavelength is actually unstable [25]. Here we will design the electric field and the period of crystal, driven by the optimal shortcuts [17–19], to achieve short-length and robust polarization devices with respect to different variations.

2. Model

Our starting point is the linear polarization state control on the basis of electro-optic effect of PPLN [21,24], see Fig. 1. To have an insight into the polarization state evolution in PPLN, a polarization coupled-mode theory is established, and the coupled wave equations of the ordinary and extraordinary waves are written as

$$\frac{dA_1}{dx} = -i\kappa A_2 e^{i\Delta\beta x}, \tag{1}$$

$$\frac{dA_2}{dx} = -i\kappa^* A_1 e^{-i\Delta\beta x}, \tag{2}$$

with $\Delta\beta = (\beta_1 - \beta_2) - G_m$, $G_m = 2\pi m/\Lambda$, and

$$\kappa = i\kappa_0 = -\frac{\omega}{2c}\frac{n_0^2 n_e^2 \gamma_{51} E}{\sqrt{n_0 n_e}}\frac{i(1-\cos m\pi)}{m\pi} \quad (m = 1,3,5...),$$

where A_1 and A_2 are the normalized amplitudes of the ordinary and extraordinary waves, respectively; $\beta_1 = 2\pi n_o/\lambda_0$ and $\beta_2 = 2\pi n_e/\lambda_0$ are the corresponding wave vectors (λ_0 is the wavelength of light); G_m is the m-th reciprocal vector, Λ is the period of PPLN crystal, n_o and

#220049 - $15.00 USD Received 29 Jul 2014; revised 8 Sep 2014; accepted 10 Sep 2014; published 25 Sep 2014

n_e are the refractive indices of ordinary and extraordinary waves, respectively; γ_{51} is the electro-optic coefficient, E is the intensity of electric field along y direction. In the following calculations, the parameters from experiments are chosen to be $\lambda_0 = 1494.8\ nm$, $\gamma_{51} = 32 \times 10^{-12}\ m/V$, $n_o = 2.214$, $n_e = 2.140$ [22,23], and $m = 1$ for simplicity.

In analogy to the time-dependent Schrödinger equation ($\hbar \equiv 1$) for two-level quantum systems, the above coupled wave equation (1) can be rewritten as, $d\mathbf{A}/dx = -i\mathbf{H_0}(x)\mathbf{A}$, with $\mathbf{A} = [A_1, A_2]^{\mathrm{T}}$ and

$$\mathbf{H_0}(x) = \begin{bmatrix} 0 & \kappa e^{i\Delta\beta x} \\ \kappa^* e^{-i\Delta\beta x} & 0 \end{bmatrix}. \tag{3}$$

Applying the rotating wave approximation, we write Hamiltonian $\mathbf{H_0}(x)$ in the interaction picture as follows,

$$\mathbf{H}(x) = \frac{1}{2}\begin{bmatrix} \Delta & -i\Omega \\ i\Omega & -\Delta \end{bmatrix}, \tag{4}$$

where $\Delta = \Delta\beta$ and $\Omega = -2\kappa_0$ play the same role of detuning and (real) Rabi frequency in quantum optics. In general, Rabi frequency $\Omega(x) \equiv \Omega$ and detuning $\Delta(x) \equiv \Delta$ are spatial dependence, which are determined by the following electric field

$$E = \frac{c}{\omega}\frac{\Omega\sqrt{n_0 n_e}}{n_0^2 n_e^2 \gamma_{51}}\frac{m\pi}{(1-\cos m\pi)}, \tag{5}$$

and the period of PPLN crystal

$$\Lambda = \frac{2\pi m}{\beta_1 - \beta_2 - \Delta}. \tag{6}$$

In what follows we will focus on how to design the x-dependent electric field and period of PPLN crystal to achieve perfect polarization conversion within short length, by assuming the input light is the extraordinary wave i.e. $A_1(0) = 0$ and $A_2(0) = 1$.

When the detuning $\Delta = 0$, that is, $\Delta\beta = (\beta_1 - \beta_2) - G_m = 0$ ($m = 1,3,5...$), the reciprocal vector totally compensates for the wave vector mismatch between ordinary and extraordinary waves. In this case, the QPM condition is satisfied, thus the period of domain inversion is $\Lambda_m = m\lambda_0/(n_o - n_e)$. Meanwhile, when the static electric field is applied, the Rabi frequency Ω, proportional to the electric field, is constant. As a result, the power exchange between the extraordinary and ordinary waves behaves like Rabi oscillation driven by the flat π pulse in quantum optics. Complete conversion can be achieved for the crystal length, $L = n\pi/\Omega$ ($n = 1,2,3...$). The resonant scheme for $n = 1$ gives the minimal length $L = 2.18\ mm$ for complete polarization conversion, when the electric field is $E = 1.63\ kV/mm$. The shorter device with $L = 0.46\ mm$ can be further achieved when the electric field is increased up to $E = 7.66\ kV/mm$. However, the resonant scheme is very sensitive to the wavelength variation, temperature fluctuation and length error. With such property, QPM technique actually provides the advantage to design tunable wavelength filter [22].

On the other hand, when the adiabatic condition,

$$\left|\frac{2\kappa_0\dot{\Delta\beta} - 2\dot{\kappa_0}\Delta\beta}{(4\kappa_0^2 + \Delta\beta^2)^{3/2}}\right| \ll 1, \tag{7}$$

is satisfied, one can convert the polarization state from the extraordinary wave to the ordinary wave along one of the instantaneous eigenstates of Hamiltonian in Eq. (4). We take Landau-Zener (LZ) scheme as an example, that is, linearly x-dependent detuning with $\Delta = \alpha(x/L - 1/2)$

#220049 - $15.00 USD Received 29 Jul 2014; revised 8 Sep 2014; accepted 10 Sep 2014; published 25 Sep 2014

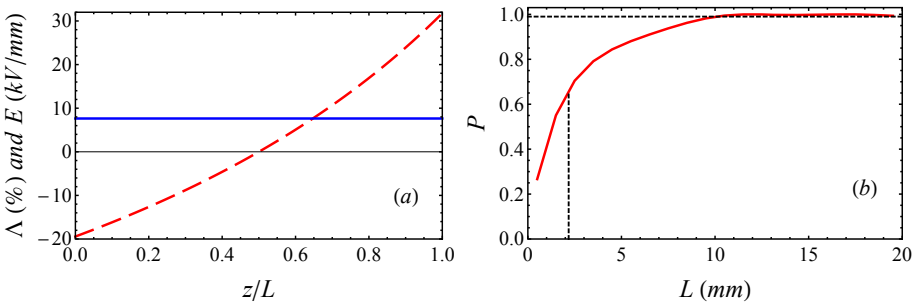

Fig. 2. (a) Functions of electric field E (solid blue line) and the period of PPLN crystal Λ (dashed red line) for LZ protocol, where Λ is re-scaled by $(\Lambda-\Lambda_1)/\Lambda_1$ with $\Lambda_1 = 20.2\ \mu m$. $L = 2.18\ mm$, $E = 7.66\ kV/mm$, and other parameters are in the maintext. (b) Dependence of conversion efficiency on the device length, where $P = 0.65$ at $L = 2.18\ mm$, and $L \geq 10$ mm for $P > 0.99$.

and a constant Rabi frequency, see Fig. 2(a). Based on the adiabatic condition (7), the crystal length requires $L \geq 10mm$ to achieve high conversion efficiency (≥ 0.99), when $\alpha = 1.5\times 10^5$ and $E = 7.66\ kV/mm$ are chosen. As compared to resonant scheme, the slow adiabatic protocol is more robust against the wavelength variation and length error, but requires longer crystal length with the same maximal value of electric fields. Figure 2 show the spatial dependence of electric field and period of PPLN crystal, and the conversion efficiency versus device length L. Obviously, when the short-length device with $L = 2.18\ mm$ is chosen, the adiabatic condition is not satisfied and conversion efficiency is only $P = 0.65$. The adiabatic technique requires the polarization rotator with longer length of device, that is, $L \geq 10\ mm$ for a given maximal value of electric field, $E = 7.66\ kV/mm$, see Fig. 2(b).

3. Dynamical invariant and optimization

Next, we shall apply STA to design the polarization rotation with high conversion efficiency but within a short length of crystal. To this end, we shall engineer the electric field and period of PPLN crystal in terms of invariant dynamics. The dynamical invariant $\mathbf{I}(x)$ can be parameterized by [17, 18],

$$\mathbf{I}(x) = \frac{\Omega_0}{2}\begin{bmatrix} \cos\theta & \sin\theta e^{-i\beta} \\ \sin\theta e^{i\beta} & -\cos\theta \end{bmatrix}, \tag{8}$$

with the eigenvalue $\varepsilon_\pm = \pm\Omega_0/2$ (Ω_0 is an arbitrary constant with units of mm^{-1}), and the eigenstates

$$|\phi_+(x)\rangle = \begin{pmatrix} \cos(\theta/2)e^{-i\beta} \\ \sin(\theta/2) \end{pmatrix}, \tag{9}$$

$$|\phi_-(x)\rangle = \begin{pmatrix} \sin(\theta/2) \\ -\cos(\theta/2)e^{i\beta} \end{pmatrix}. \tag{10}$$

The solution of Schrödinger equantion, $i\hbar\partial_x\Psi(x) = \mathbf{H_0}\Psi(x)$, can be presented as the superposition of eigenstates of dynamical invariant [16], $|\Psi(x)\rangle = \sum_\pm c_\pm e^{i\gamma_\pm(x)}|\phi_\pm(x)\rangle$, where $c_\pm$ are x-independent amplitudes and the Lewis-Riesenfeld phase $\gamma_\pm$ satisfies

$$\dot\gamma_\pm(x) = \pm\frac{1}{2}\left(\dot\beta - \frac{\dot\theta\tan\beta}{\sin\theta}\right). \tag{11}$$

#220049 - $15.00 USD Received 29 Jul 2014; revised 8 Sep 2014; accepted 10 Sep 2014; published 25 Sep 2014

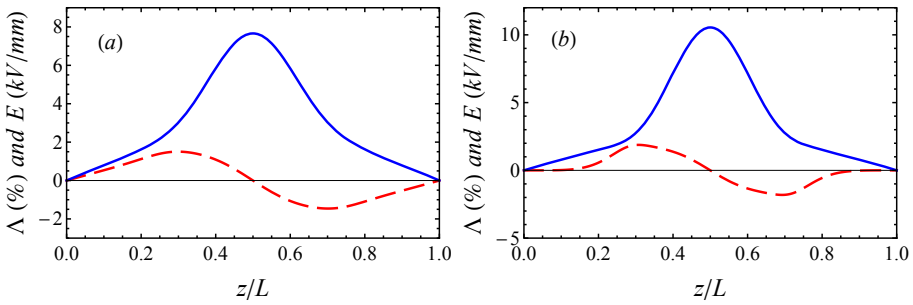

Fig. 3. Functions of electric field E (solid blue line) and the period of PPLN crystal Λ (dashed red line) for Δ-optimal (a) and Ω-optimal (b) protocols designed by shortcuts to adiabaticity, where $L = 2.18$ *mm* and other parameters are the same as those in Fig. 2.

The invariant condition, $\partial_x \mathbf{I} - (1/i)[\mathbf{H}, \mathbf{I}] = 0$, gives

$$\Omega = -\dot{\theta}/\cos\beta, \tag{12}$$

$$\Delta = \dot{\beta} + \dot{\theta}\tan\beta\cot\theta, \tag{13}$$

allowing us to design the electric field and period of the PPNL crystal by Eqs. (5) and (6).

Our goal is to achieve complete polarization state conversion from the extraordinary wave at $x = 0$ to the ordinary wave at $x = L$, within short crystal length. So our initial and final states are assumed to be $|\Psi(0)\rangle \equiv |1\rangle = \binom{0}{1}$ and $|\Psi(L)\rangle \equiv |2\rangle = \binom{1}{0}$. Supposing the polarization state evolution follows the eigenstate, $|\phi_+\rangle$, of dynamical invariant, we can set the following boundary conditions:

$$\theta(0) = \pi \ \text{ and } \ \theta(L) = 0. \tag{14}$$

In general, if the polarization rotation is desired to be from initial angle θ_i to arbitrary angle θ_f, rather than at 90°, the initial and final boundary condition can be further modified as $\theta(0) = \theta_i$ and $\theta(L) = \theta_f$. In addition, the commutativity between $\mathbf{H}$ and $\mathbf{I}$ at the boundaries gives more boundary conditions,

$$\dot{\theta}(0) = 0, \quad \dot{\theta}(L) = 0, \tag{15}$$

which implies that the polarization states at input $x = 0$ and output $x = L$ can transform into the eigenstates of $\mathbf{I}(z)$ smoothly. There is still much freedom to design Ω and Δ (finally E and Λ), see Eqs. (12) and (13), by choosing arbitrary functions of θ and β except at the boundaries. The freedom allows one to engineer stable or robust system evolution against different errors [17–19].

3.1. Δ-optimal protocol

First of all, we shall concentrate on the robust polarization rotation with respect to input wavelength/relative refractive index variations, since in the experiment the parameters like the central wavelength λ_0 for QPM condition and refractive index are unstable due to the temperature fluctuation or other perturbations [22,25]. The dominant effect of input wavelength/relative refractive index variations can be simply described by the systematic frequency error in diagonal terms of Hamiltonian (4), that is, $\mathbf{H}' = \delta\sigma_z$, where σ_z is Pauli matrix, and the amplitude of systematic errors δ is $\delta \simeq 2\pi(n_0 - n_e)\delta\lambda/\lambda_0^2$ or $\delta \simeq 2\pi\delta n/\lambda_0$. In the error-free case, we consider the family of protocols that results in perfect polarization conversion from the extraordinary

#220049 - $15.00 USD Received 29 Jul 2014; revised 8 Sep 2014; accepted 10 Sep 2014; published 25 Sep 2014

wave, $|1\rangle$, to the ordinary wave, $|2\rangle$: the unperturbed solution, $|\Psi(x)\rangle = e^{i\gamma_+(x)}|\phi_+(x)\rangle$, satisfying Eq. (14). Considering $\mathbf{H}'$ as perturbation, we define the wavelength/refractive index-error sensitivity as [17, 18]

$$q_\Delta = -\frac{1}{2}\frac{\partial^2 P(L)}{\partial \delta^2}\bigg|_{\delta=0}, \tag{16}$$

where P is conversion coefficient, which is the output power of ordinary wave at $z = L$, i.e. $P \approx 1 - q_\Delta \delta^2$. Using perturbation theory and keeping the second order, we finally obtain

$$q_\Delta = \frac{1}{4}\left|\int_0^L dx \sin\theta e^{im(x)}\right|^2, \tag{17}$$

with $m(x) = -2\gamma_+(x) + \beta(x)$. To nullify q_Δ, i.e. $q_\Delta = 0$, we assume $m(x) = 2\theta + 2\zeta\sin(2\theta)$, and solve for free parameter ζ [18, 19]. As an example, we may choose

$$\theta = \frac{\pi}{2}\left[1 - \sin\frac{\pi(2x-L)}{2L}\right], \tag{18}$$

and β can be solved as

$$\beta = \sin^{-1}\left(\frac{2M\sin\theta}{\sqrt{1+4M^2\sin^2\theta}}\right). \tag{19}$$

with $M = 1 + 2\zeta\cos(2\theta)$. Combining Eqs. (18) and (19), we solve for the design parameters as follows

$$\Omega = -\dot{\theta}\sqrt{1+4M^2\sin^2\theta}, \tag{20}$$

$$\Delta = 2\dot{\theta}\cos\theta\left[M + \frac{1-4\zeta+6\zeta\cos(2\theta)}{1+4M^2\sin^2\theta}\right], \tag{21}$$

which finally gives $q_\Delta = 0$ with the parameter $\zeta = -0.206$. The electric field and the period of PPLN crystal are eventually calculated from Eqs. (5) and (6), see Fig. 3(a). For the designed shortcuts, the maximal value of Rabi frequency is calculated as,

$$\Omega_{max} = \frac{\sqrt{1+4(1-2\zeta)^2\pi^2}}{2L} \propto \frac{1}{L}, \tag{22}$$

which provides the corresponding maximal value of electric fields as follows,

$$E_{max} = \frac{\pi c}{2\omega}\frac{\Omega_{max}\sqrt{n_0 n_e}}{n_0^2 n_e^2 \gamma_{51}}. \tag{23}$$

Clearly, the electric field, E_{max}, is proportional to $1/L$, as shown in Fig. 4, which means the driven electric field will increase when shortening the device length. Therefore, the physical constraint on the driven electric field will set the limit of device length, L, though any arbitrarily short-length polarization rotation can be ideally achieved by using shortcuts to adiabaticity with right boundary conditions (14). The larger driven electric field with the magnitude of $E = 7.66$ kV/mm can be implemented in the technique proposed by Thaniyavarn [20] to make the device shorter, though the usual polarization devices in PPLN systems require much smaller driven electric fields with the magnitude of $E = 0.1$ kV/mm [25].

Figure 5(a) illustrates the robustness of conversion efficiency against input wavelength in 2.18 mm crystals. Clearly, Δ-optimal protocol is more robust than the resonant scheme, obtained from QPM condition, In Fig. 5(a) we see that the full width ratio at half maximum

#220049 - $15.00 USD Received 29 Jul 2014; revised 8 Sep 2014; accepted 10 Sep 2014; published 25 Sep 2014

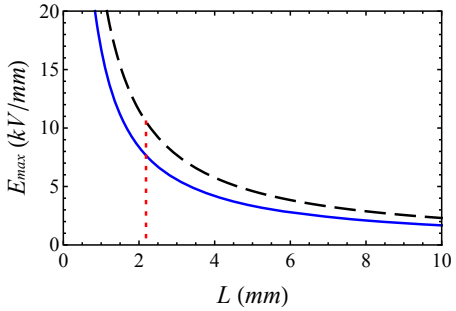

Fig. 4. Dependence of E_{max} on the device length L for Δ-optimal (solid blue line) and Ω-optimal protocols (black dashed line), where the dotted red line corresponds to the parameters $L = 2.18$ mm and $E_{max} = 7.66\ kV/mm$ used in the protocol of Fig. 2(a).

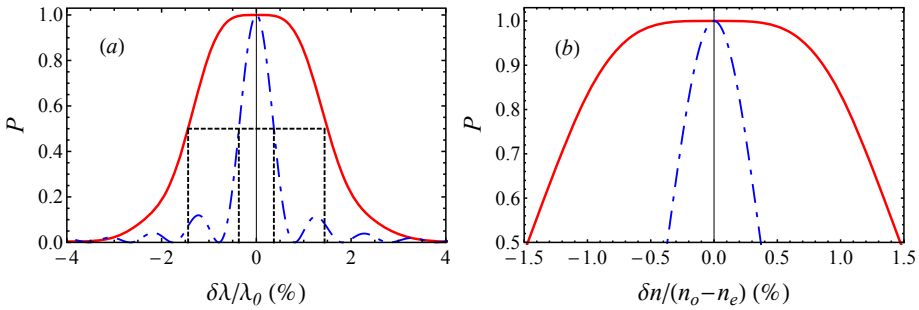

Fig. 5. Conversion efficiency versus input wavelength (a) and relative refractive index (b) variations for Δ-optimal protocol (solid red line) and resonant protocol (dotted-dash blue line). $L = 2.18\ mm$ and other parameters are the same as those in Fig. 2.

of conversion efficiency, $\delta\lambda/\lambda_0$, is increased from 0.74% for QPM scheme up to 2.88% for shortcut scheme. With high-order cancellation, more robust protocol can be further designed to make spectrum width broader [19]. Therefore, this result can be applicable to design broadband spectrum polarization devices. In addition, as compared to the resonant scheme obtained from QPM condition, Fig. 5(b) also shows that the deigned shortcuts is more stable with respect the relative refractive index variation induced by temperature fluctuation. Usually, the refractive indices (n_0 and n_e) are temperature dependent, so that to design more robust polarization devices with respect to the derivation of birefringence is useful to have better tolerance with respect to the temperature fluctuation. In the experiment [22], the derivation of birefringence can be calculated from $\delta n/\delta T = (1/\Lambda_1)d\lambda/dT$, where the wavelength-tuning rates to temperature are measured as $d\lambda/dT = -0.422\ nm/^{\circ}\mathrm{C}$ for PPLN and and $d\lambda/dT = -24\ nm/^{\circ}\mathrm{C}$ for PPLT. So the stability with respect to temperature fluctuation becomes more significant when PPLN is replaced by PPLT.

3.2. Ω-optimal protocol

Next we turn to the optimization of shortcuts for robust polarization rotation with respect to the driven electric fields, which only affects Rabi frequency, based on Eq. (5), and thus can be described as $\mathbf{H}' = \delta\sigma_y$, where σ_y is Pauli matrix, and the amplitude of error is $\delta = (2\omega/\pi c)(n_o^2 n_e^2 \gamma_{51}/\sqrt{n_o n_e})\delta E$. Similarly, we use the perturbation theory and obtain the

#220049 - $15.00 USD Received 29 Jul 2014; revised 8 Sep 2014; accepted 10 Sep 2014; published 25 Sep 2014

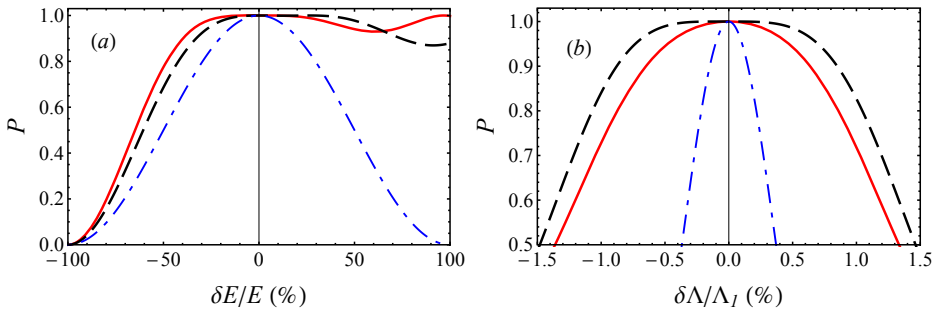

Fig. 6. Conversion efficiency versus electric field (a) and crystal period (b) variations for Ω-optimal protocol (solid red line), Δ-optimal (black dashed line) and resonant protocols (dotted-dash blue line). $L = 2.18\ mm$ and other parameters are the same as those in Fig. 2.

electric field-error sensitivity

$$q_\Omega = \frac{1}{4}\left|\int_0^L dx\dot{\theta}\sin^2\theta e^{im(x)}\right|^2, \tag{24}$$

in the second order approximation. Following [17], we can impose $m(x) = 2\theta - \sin(2\theta)$, so that

$$\beta = \arctan(4\sin^3\theta), \tag{25}$$

to make $q_\Omega = 0$. In this case, Eqs. (20) and (21) are valid when $\zeta = -0.5$, which finally give the period of PPLN crystal and electric field, as shown Fig. 3(b). The profiles of the period of PPLN crystal and electric field for Ω-optimal protocol are similar to those for Δ-optimal protocol, but we can see from Eqs. (22) and (23) that the maximal values of electric fields are larger, see Fig. 4. In the following discussion, we will make the comparison for the different protocols with the same length $L = 2.18\ mm$.

Figure 6(a) demonstrated that Ω-optimal protocol is more stable with respect electric field variation than the resonant scheme, obtained from QPM technique. Since the fluctuation of electric field is descried by the symmetric error in Rabi frequency, Ω-optimal protocol has better tolerance than Δ-optimal one, especially when the actual fields are less than the desired ones. In fact, the robustness against electric field variation is extremely important for our shortcut schemes, since all protocols designed here require special spatial dependence of electric fields, which could make the experiments more complicated. Similarly, both Ω-optimal and Δ-optimal protocols are more insensitive than the resonant scheme with respect to the error in period of crystal, Λ, see Fig. 6(b). In this case, Δ-optimal protocol is better than Ω-optimal one, since the fluctuation of crystal period is nothing but the symmetric frequency error in detuning. Finally, we would like to mention that Δ-optimal and Ω-optimal protocols can somehow improve the stability of conversion efficiency with respect to length error, and thus they are more robust than the resonant schemes [15], since the length-scaling errors are formally reduced to systematic errors of the Hamiltonian, in both Rabi frequency and detuning terms [27].

4. Conclusions

To conclude, we propose short-length and robust polarization rotators in PPLN crystal by using shortcuts to adiabaticity. The electric field and period of PPLN crystal are designed to optimize the stability with respect to input wavelength/refractive index variations. In addition, the stability of conversion efficiency with respect to the fluctuation of electric field and crystal period are

#220049 - $15.00 USD Received 29 Jul 2014; revised 8 Sep 2014; accepted 10 Sep 2014; published 25 Sep 2014

also discussed. As an example, our shortcuts presented here are designed to polarization conversion from extraordinary wave to ordinary wave from $x = 0$ to $x = L$. Actually, by changing the initial and finally boundary conditions, we can further realize the arbitrary control of polarization states, which are applicable to other polarization devices, such as polarization splitter and polarization-state generator. Last but not least, the electric field and period of crystal length are in principle feasible with state-of-the-art technologies, but the details of experimental implementation are worthwhile for a separate study.

Acknowledgments

This work was partially supported by the NSFC (11474193, 61404079 and 61176118), the Shanghai Rising-Star, Pujiang, and Yangfan Program (12QH1400800, 13PJ1403000 and 14YF1408400), the Specialized Research Fund for the Doctoral Program (2013310811003), the Program for Eastern Scholar, and the MOST of Taiwan (103-2221-E-006-055 and 103-3113-M-110-001).

#220049 - $15.00 USD Received 29 Jul 2014; revised 8 Sep 2014; accepted 10 Sep 2014; published 25 Sep 2014